Multiphysics Modeling and Driving Strategy Optimization of an Urban-Concept Vehicle

J.-C. Olivier, G. Wasselynck, D. Trichet, N. Bernard, S. Hmam
Nantes University
IREENA (EA 4642)
Nantes, France
Email: jean-christophe.olivier@univ-nantes.fr

S. Chevalier, C. Josset, B. Auvity
Polytechnic School of Nantes University
LTN (CNRS-UMR 6607)
Nantes, France
Email: bruno.auvity@univ-nantes.fr

Gaetano Squadrito
CNR-ITAE
Messina, Italy
Email: gaetano.squadrito@itae.cnr.it

***Abstract*—This paper is dedicated to the optimization of the driving strategy of a high efficiency fuel cell based power train. This power train is developed to equip an urban-concept vehicle that runs energetic races where the objectives are to go the furthest with the lowest quantity of fuel (Shell Eco Marathon). Through a comprehensive dynamical model, including the mechanical requirement, the thermal behavior of the fuel cell stack and the various losses and consumption of the power train devices. This model is then integrated into a global optimization algorithm, to determine the best race strategy to be adopted (velocity profile, motor current, gearbox ratio).**

***Keywords*—fuel-cell, power train, multiphysics modeling, energy optimization**

I. Introduction

Given the new economic and ecological issues, car manufacturers should focus on alternative energy sources, such as electric batteries or fuel cells [1]–[6]. Although still young and hard to handle, fuel cells, and particularly Proton Exchange Membrane Fuel Cell (PEMFC), remain a promising way. Indeed, a hydrogen fuel cell vehicle has naturally a better performance than a diesel car (usually 30 % against 22 % of efficiency at the wheel). Moreover, the energy supplied by the fuel cell is electric, which allows propulsion chains more flexible with high performances [7]. For several years, a prototype vehicle with extremely low energy consumption has been developed by researchers and electrical engineering students, to run energetic races [8]–[10]. The energy source of this vehicle is a Proton Exchange Membrane Fuel Cell (PEMFC). From 2010 to 2012, this vehicle has been recognized by the Shell group (through the 2010 edition of the Shell Eco-marathon competition, on the EuroSpeedway race track, Germany) as the world most energy efficient car, with an equivalent consumption of only 0.02 litres of unleaded gasoline 95 per 100 km, at a minimum average speed of 30 km/h.

Since 2013, a new car with extremely low energy consumption is developed (see Figure 1). It comes under the urban-concept category, which aims to promote the development of vehicles closest to true city cars. The energy source of this vehicle is also a PEMFC. To achieve an energy consumption as low as possible, each element of the vehicle must be optimized, from the mechanical angle (drag coefficient, frontal area, slop, road-wheel friction, weight) to the electrical architecture (power converter and motor efficiencies and fuel cell accessories consumption). This optimisation has been done in previous works, but without taking into account the driving strategy [8]. In this paper, the optimal driving strategy that minimizes the car energy demand is presented. It is based on a multi-physics modeling of the power train, taking into account the road profil and the race constraints (average speed, stop at each turn, etc.) [11]–[13]. This model is then integrated into a global optimization algorithm, which lead to the best velocity profile, motor current and gearbox ratio.

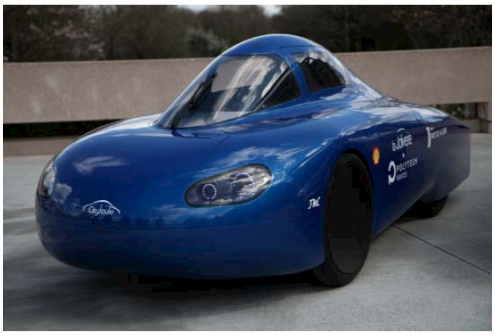

Fig. 1. The Urban-Concept vehicle Cityjoule.

The paper is organized as follows: In section II, the vehicle specifications and the race characteristics are presented. A focus is made on power train architecture from the fuel cell stack to the mechanical needs. In section III, a dynamical and multi-physics model is developed. In this section, each part of the power train is presented. An originality of this work is the addition of a thermal modeling of the PEMFC, in order to take into account the auxiliary stack consumption in energy balance, including the air feeding and cooling systems. The optimisation results are given in Section IV, which allow to achieve a driving strategy minimizing the final energy consumed by the vehicle. In the final paper, simulations and experimental results are compared to a real race, recorded during the previous edition of the Shell eco-marathon, in Rotterdam, Netherlands. Conclusions are given in Section V.

II. Presentation of the Race and Vehicle Characteristics

The urban-concept car and its associated fuel cell power train have been both designed and built to participate to the

978-1-4673-7637-2/15/$31.00 ©2015 IEEE

Shell Eco Marathon energetic race (Rotterdam, Netherlands). The principle of such a competition is to drive a vehicle with one pilot the furthest with the lowest quantity of fuel at a minimum average speed of 25 km/h. A minimum weight of 70 kg is imposed for the pilot. Each competitor will have to travel 10 turns of the race track corresponding to 16.1 km in less than 40 minutes. In the urban-concept category, a stop is mandatory during at each lap. To evaluate prototype car efficiency, the fuel quantity carried on board is measured before and after the attempt. Wide range of fuels can be used (Unleaded gasoline; diesel; LPG; GTL; fatty acid methyl ester; ethanol E100 and hydrogen). In our fuel cell category, an official flow meter is used to measure the volume of hydrogen consumed during the attempt. This amount of energy is converted into kilometers per kWh. It is important to notice that in the fuel cell category, battery is not allowed in the car except for safety purposes, i.e. to power the car-horn and the hydrogen sensor.

III. Multi-Physics modeling of the powertrain

In this section, a dynamical model of the vehicle is proposed. For a set of input parameters (e.g. motor current, road slope, ambient temperature,...) this model calculates the evolution of the various system states, the losses and the consumption of each subsystem (see Figure 2). This model

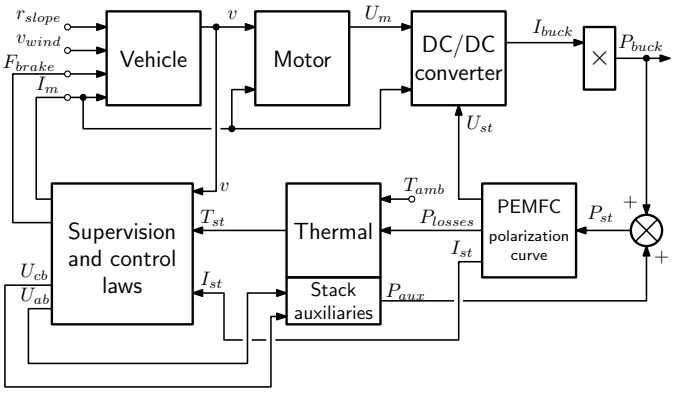

Fig. 2. Tank-to-wheel model.

is organized around six main blocks: The mechanical part, the propulsion motor, the power converter, the fuel cell, the stack accessories coupled to a thermal model, and the control laws and supervision. This dynamical model is oriented towards the optimization and must be solved quickly. Thus, only the velocity v and the stack temperature T_{st}, which are the slowest variables, are taken into account. All other dynamics are considered fast enough to be regarded as instantaneous.

The urban-concept *Cityjoule* presented in this paper is made of two identical power trains, each supplying one of the two rear wheels. In the next sections, only one power train is studied.

In a previous work, the modelization of the ironless DC-motor, the power converter and the fuel cell have already been developed [8]. Therefore, this work focuses on the other parts of the system, i.e. the mechanical and thermal modeling, the driving and auxiliary management laws.

A. Mechanical model

In order to obtain the dynamical behavior of the vehicle, the mechanical equations must be solved. To run, the vehicle has to overcome the efforts due to the aerodynamic F_{aero}, the slope F_{slope} and the rolling resistance due to friction between the wheel and the road F_{rr}. The fundamental law of the mechanic gives the next equation to solve (see Figure 3) [13]:

$$m\frac{d\,v(t)}{dt} = F_w - F_{rr} - F_{slope} - F_{aero} - F_{brake} \qquad (1)$$

where m is the mass of the vehicle, F_w is the propulsion force applied to wheel through the electrical motor and F_{brake} the mechanical braking force.

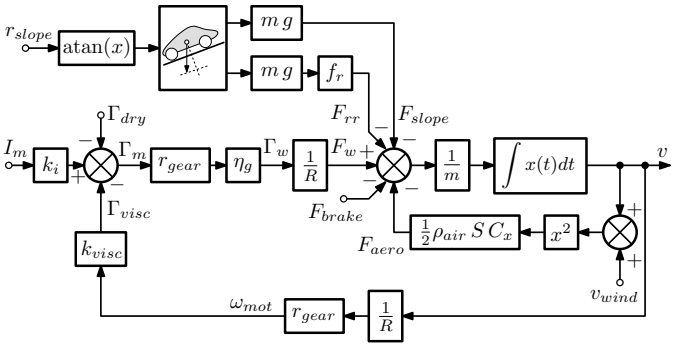

Fig. 3. Dynamical model of the mechanical part of the vehicle.

The aerodynamic force F_{aero} is computed from the mechanical parameters of the vehicle and the wind speed v_{wind} :

$$F_{aero} = \frac{1}{2}\rho_{air} S\, C_x \left(v(t) + v_{wind}\right)^2 \qquad (2)$$

with ρ_{air} the mass density of air, C_x the drag coefficient, S the frontal area, $v(t)$ and v_{wind} respectively the vehicle and wind velocities (in m.s^{-1}). The forces due to the rolling resistance and the road inclination are calculated from the mass m of the vehicle and the slope r_{slope} given in % :

$$F_{rr} = m\,g\,f_r\,\cos\left(\arctan\left(r_{slope}\right)\right) \qquad (3)$$

$$F_{slope} = m\,g\,\sin\left(\arctan\left(r_{slope}\right)\right) \qquad (4)$$

The total drive Force F_w applied through both rear wheels is calculated from the motor torque Γ_m, such as:

$$F_w = \eta_g \frac{r_{gear}}{R}\,\Gamma_m \qquad (5)$$

where R is the wheel radius, r_{gear} the gearbox ratio of the transmission and η_g its efficiency.

B. Thermal model of the fuel cell stack

The typical nominal power of a powertrain for an urban-concept car is below 1 kW. For such relatively low power need, the auxiliary devices of the system play a crucial role in the total energy consumption. It is well known that fuel cell stack auxiliaries cause a drop in system efficiency at low power. It is therefore necessary to take their consumption into account [11], [14]–[16]. For this vehicle, the accessories of the fuel cell are limited to a air blower and a cooling fan. The operation and the consumption of these accessories are presented in this section. The thermal source $P_{th\,src}$ due to the

irreversibilities of the electrochemical reaction, is evacuated through many different paths. In this work, it is considered that thermal evacuation is achieved by the air flow rate in fuel cell channels $P_{th\,ab}$, the liquid-vapor phase change $P_{th\,stm}$ of the water produced by the electrochemical reaction of the fuel cell, the natural convection $P_{th\,nat}$ and the forced convection assured by the cooling blower $P_{th\,cb}$. Thus, a dynamical thermal model can be expressed by next equation [17], [18]:

$$m_{fc} C_p \frac{d\,T_{st}}{dt} = P_{th\,src} - P_{th\,ab} - P_{th\,stm} - P_{th\,nat} - P_{th\,cb} \quad (6)$$

The thermal source $P_{th\,src}$ is calculated from the total power supplied by the PEMFC and its polarization curve:

$$P_{th\,src} = (n_{cells}\,E_{Nernst} - U_{st})\;I_{st} \quad (7)$$

where E_{Nernst} is the reversible voltage of a cell, calculated from the Nernst equation [19], [20] and n_{cells} the number of cells.

The air flow in the air channel, produced by the air blower, permits to evacuate a part of the heat by forced convection. The air flow $Q_{v\,ab}$ (in $l.min^{-1}$), for given Stoechiometric-ratio S_c and stack current I_{st}, is given by next equation:

$$Q_{v\,ab} = 60000\,\frac{5\,R_c\,(273,15 + T_{st})}{4\,P_a\,F}\,I_{st}\,n_{cells}\,S_c \quad (8)$$

with R_c the ideal gas constant (8.31 J.mol^{-1}.K^{-1}, T_{st}) the stack temperature (in °C) and P_a the atmospheric pressure (101300 Pa). By assuming a perfect exchange between the air channel and the stack, the output of air temperature is equal to the mean stack temperature T_{st}. Moreover, the input air temperature is equal to the ambient T_{amb}. Then the evacuated thermal power is:

$$P_{th\,ab} = \frac{1}{60}\rho_{air}\,Q_{v\,air}\,C_{p\,air}\;(T_{st} - T_{amb}) \quad (9)$$

where ρ_{air} is the air density (1.2 kg.m^{-3}), $C_{p\,air}$ its specific heat (1000 J.K^{-1}kg^{-1}).

The water produced during the electrochemical reaction in liquid form [20], [21]. Assuming that this water is completely drained through the air channel in vapor form, the power drained by the liquid-vapor phase change is given by:

$$P_{th\,stm} = \dot{m}_{H2O}\,L_{H2O} \quad (10)$$

where $\dot{m}_{H2O}$ is the water mass flow-rate (g.s^{-1}) evacuated through the air channel and L_{H2O} the latent heat of vaporization (2500 kJ.kg^{-1}). The amount of water produced by the reaction depends only on the stack current I_{st} provided by the fuel cell. The flow-rate $\dot{m}_{H2O}$ is then given by the following equation:

$$\dot{m}_{H2O} = n_{cells}\frac{R_c\,(273.15 + T_{st})}{4\,P_a\,F}I_{st} \quad (11)$$

The natural convection exchange coefficient is deduced from experimental measurements and expressed as :

$$P_{th\,nat} = k_{nat}\,(T_{st} - T_{amb}) \quad (12)$$

The last term of the equation (6) is the forced convection by the cooling blower. For the studied fuel cell stack, each cell is separated from the other by a corrugated iron sheet. Knowing the air flow-rate $\dot{m}_{cb}$ and considering a perfect exchange with the fuel cell, the thermal power evacuated by the cooling blower is given by:

$$P_{th\,cb} = \rho_{air}\,Q_{v\,cb}\,C_{p\,air}(T_{st} - T_{amb}) \quad (13)$$

Now that each part of the thermal model was described, its coupling with the electrical model of the fuel cell stack and accessories must been done. From the stack current I_{st} and temperature T_{st}, equations (9), (10) and (12) can be directly calculated. For equation (13), the air flow rate is an input parameter for the model. In this work, it is considered that the cooling blower is controlled through its voltage U_{cb}. The same assumption is made for the control of the air blower (U_{ab}).

The air flow rate of the cooling blower and air feeding fan are measured on a fuel-cell stack made of 28 cells (31 cm^2 of active area) manufactured by the society *MES*. The cooling system is a 12 V radial blower, Micronel U97 and the air feeding fan is a 12 V axial blower, Micronel D484.

Measurements on this fuel cell assembly allow to deduce the airflow and power consumption of the auxiliaries, as shown in Figure 4.

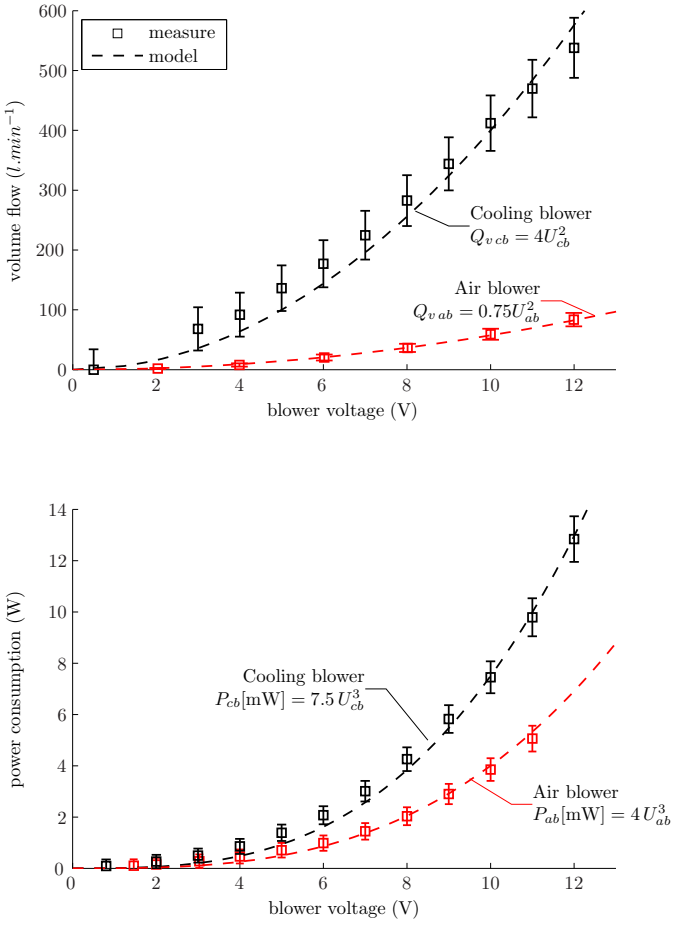

Fig. 4. Characteristics of the cooling and air blowers.

For both blower, a least squares regression is used to fit the experimental datas:

$$Q_{v\,ab} = 0.75\,U_{ab} \quad \text{and} \quad P_{ab} = 4.0\,U_{ab}^3 \tag{14}$$

$$Q_{v\,cb} = 4.00\,U_{cb} \quad \text{and} \quad P_{cb} = 7.5\,U_{cb}^3 \tag{15}$$

C. Driving and auxiliary management laws

The last part of the model to be detailed is the supervision with the control laws. These functions are performed by a microcontroller ATMEGA 128. This system receives and processes various information such as the setting motor current, stack temperature, fuel cell current, vehicle velocity, etc.

For the cooling regulation, an hysteresis controller is used. The cooling blower is turned on with a given voltage value, if the temperature exceed a threshold value T_{max} and while it remains greater than a lower value T_{min}. Even if this control law is not optimal, it has the advantage of being extremely robust with respect to changes in operating conditions (stack losses, ambient temperature, ...). Further, to smooth the power supplied by the stack, the cooling blower is supplied only during the free-wheel phase (i.e. deceleration phase), when the electrical motor is turn off and the vehicle consumption is minimum (see Figure 5).

For the driving strategy, each lap of the race can be decomposed in three sequences. The first one is a starting phase from 0 km/h to an intermediate velocity v_{min}, with a constant motor current I_{start}. During this phase, the acceleration should be high enough so as not to lose too much time for the rest of the lap. In contrast, for a too high torque applied to the wheel, the power train efficiency could be greatly reduced.

The second phase is a *constant speed* strategy. The objective is to maintain an average speed as constant as possible, with the greatest possible efficiency. In ref. [8], it is shown that the optimum efficiency is obtained by performing a series of acceleration and free wheel. The acceleration phases are carried out with the optimum torque, which maximizing the energy efficiency of the power chain. The parameters to be optimized are the motor current I_{acc} applied during the acceleration phases and speed hysteresis thresholds v_{min} and v_{max}. The optimization of these parameters must improve the global energetic performance of the vehicle.

D. Formulation of the optimization problem

For the optimization of this problem, a standard formulation is used. The objective function can be expressed has *the minimization of the fuel consumption on a full race (10 laps), under constraint of a minimum average speed of 25 km/h*: The tank-to-wheel model illustrated by Figure 2 is implemented in Matlab. The state-space variables taken into account are the velocity $v(t)$ and the stack temperature $T_{st(t)}$, according to equations (1) and (6). Both equations are computed using a 4th order Runge-Kutta ODE solver.

A particle swarm algorithm is used with five input parameters (see Figure 5), which are the motor currents I_{start} and I_{acc}, the maximum and minimum speeds v_{min} and v_{max}, and the gearbox ratio r_{gear} between the electric motor and the wheel. The tuning of the particle swarm algorithm is classical, with a population of 50 particles and a maximum number of

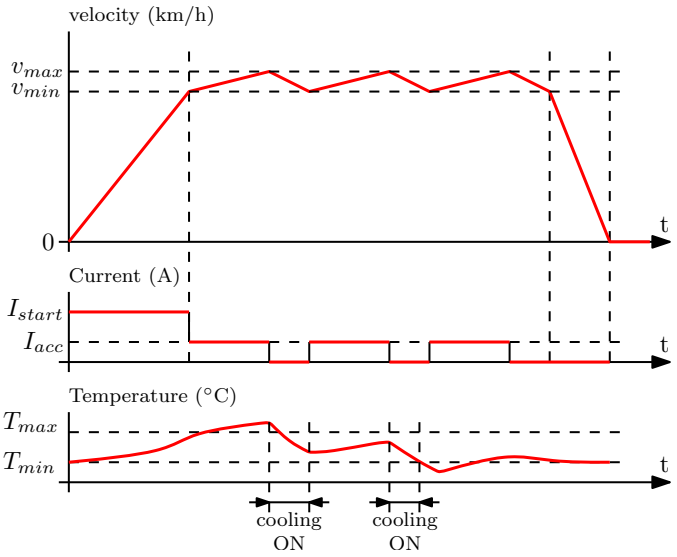

Fig. 5. Typical speed, current and temperature profiles for each lap.

iterations of 200 [22]. To sum up, the optimization problem can be formulated such as:

$$\begin{aligned} &\text{Minimize} : f(\mathbf{x}) = (\text{fuel consumption}) \\ &\text{with} : \mathbf{x} = \{I_{start}; I_{acc}; v_{min}; v_{max}; r_{gear}\} \\ &\text{subject to} : \begin{array}{l} v_{min} \leq v_{max} \\ \text{mean}\,(v(t)) \geq 25 \text{ km/h} \end{array} \end{aligned}$$

IV. Results

The optimization results for the runs of the shell eco marathon in Rotterdam is summarized by Table I. This optimisation takes into account the slope of the road and is obtained for an ambient temperature of 25°C. The list of the vehicle parameters, used for the optimization, is given by Table II. As shown in Figure 6, the vehicle is launch in 30 secondes (0-25km/h). An average speed of 27km/h is then maintained with a small velocity ripple of 1.6km/h, due to the successions of acceleration and free wheel phases. At the end the vehicle is able to brake very quickly and efficiently. During the lap, and by considering an initial temperature of 41°C, the cooling system is activated during the free wheel phases to maintain a stack temperature between 41 and 44°C.

With this set of parameters, the global tank-to-wheel efficiency for one lap of the race is greater than 45 % and an energy performance of about 500 Wh/100km (i.e. an equivalent consumption of 1 L_{SP95} for 1800 km) is achieved. This simulation result is obtained for ideal climatic conditions without wind. This performance can thus be viewed as being the maximum value to be reached by the vehicle.

Considering the thermal behavior of the fuel cell, the proposed dynamical model permits to estimate the repartition of the heat through the various possible paths (natural convection, air feeding, liquid to vapor phase, cooling system). Figure 7 gives the thermal power repartition in steady state, to maintain an average temperature of 43 degrees, as shown on Figure 6. Heat is thus mainly evacuated by the cooling system and the

TABLE I. OPTIMIZATION RESULT.

Parameter	Value
I_{start}	10.8 A
I_{acc}	3.1 A
v_{max}	27.8 km/h
v_{min}	26.2 km/h
r_{gear}	200/14
Average velocity	25.0 km/h
Fuel cell losses	3.04 Wh/lap
Motor losses	0.39 Wh/lap
DC-DC converter losses	0.23 Wh/lap
Mechanical transmission losses	0.11 Wh/lap
Supervision system consumption	0.37 Wh/lap
Mechanical energy	3.7 Wh/lap
Hydrogen consumption	7.96 Wh/lap
Tank-to-wheel efficiency	46.20 %
Performance	4.94 Wh/km
	1855.75 km/L$_{SP95}$

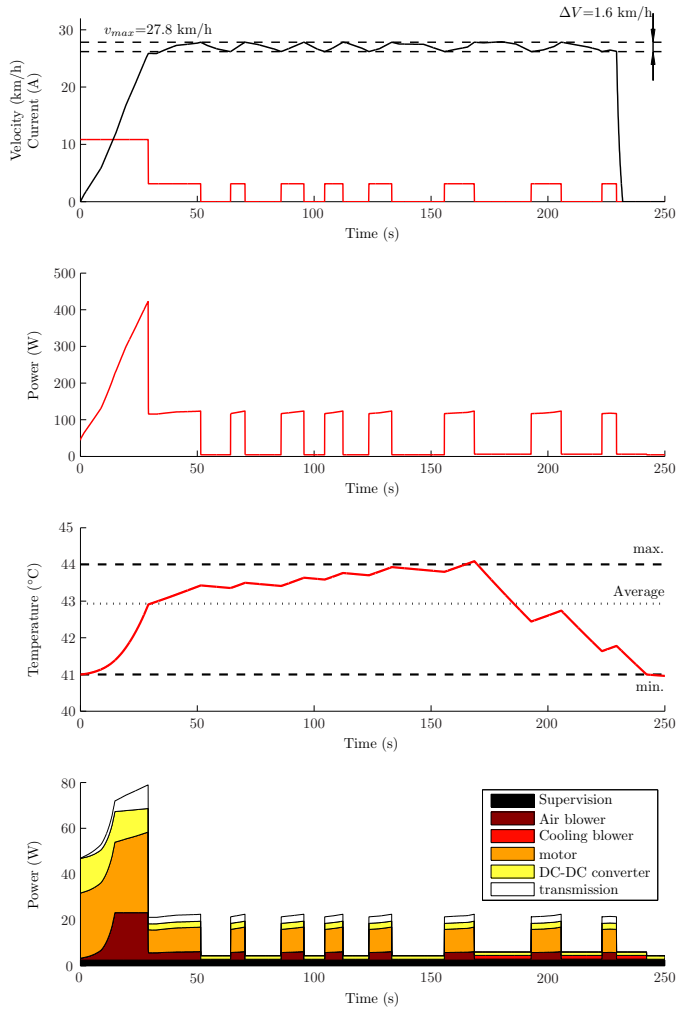

Fig. 6. Optimal profils for one lap of the Cityjoule vehicle, on the Rotterdam race.

liquid to steam phase change of the water produced by the reaction. It must be noted that the assumption of a complete conversion to steam of the water produced in liquid form is still debating by the scientific community [21], [23]–[25]. That is why in future works, experimental measurements must be done to confirm this hypothesis.

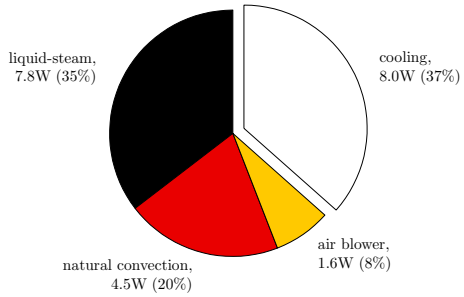

Fig. 7. Heat evacuation paths for an average temperature of 43°C.

Figure 8 presents the Sankey diagram of the powertrain for a lap. This energy diagram reveals that the main source of energy loss is the PEMFC stack: 38% of the primary hydrogen energy is lost in the electrochemical process. A total of 4.6% of the primary energy is consumed by the fuel cell stack auxiliaries, constituted by the air blower and the cooling fan. Finally, 46% of the primary hydrogen energy is available to the wheel.

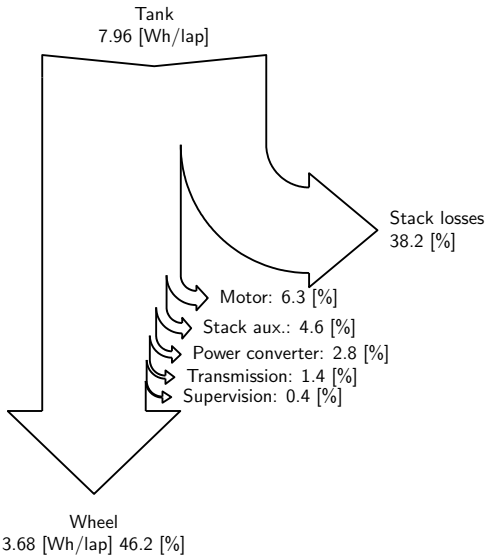

Fig. 8. Sankey diagram for one lap.

V. CONCLUSIONS

In this paper, an analytical tank-to-wheel model of an Urban-Concept fuel cell vehicle is presented. It takes into account the mechanical needs, the losses of each stage of the power train (fuel cell and auxiliaries, power converter, motor, transmission) and the dynamical thermal behavior of the fuel cell to account accurately the consumption of the fuel cell stack auxiliaries consumption. Using a set of five driving parameters (speed thresholds, gear ratio and motor currents), an optimal

driving strategy is obtained using a global optimisation algorithm. This multi-physics and dynamic model is based on the consumption and the main interactions between the various elements of the car. Therefore, the optimal driving strategy is obtained using a global optimisation algorithm which accounts for race constraints. This optimization leads to a maximum performance of 500Wh/100km for this urban vehicle, with an average speed of 25km/h. During the 2014 Shell-eco Marathon, the Polyjoule team was ranked in first place in the fuel cell category, with a performance of 660Wh/100km. In 2015, with the same vehicle and driving strategy, the team still obtained the first place, but with a performance of 800Wh/100km. This difference between these two results is mainly explained by the meteorological conditions, and especially wind, ambiant temperature and relative humidity. Then, futur works will be focus on the influence of these parameters to the vehicle performances.

TABLE II. PARAMETERS OF THE VEHICLE.

Parameter	Symbol	Value
masse	m	150kg
drag coefficient	C_x	0.1
frontal area	S	0.88m^2
air density	ρ_{air}	1.2kg.m^{-3}
rolling resistance coefficient	f_r	2.10^{-3}
transmission efficiency	η_g	0.95
number of cells	n_{cells}	28
mass of the fuel cell	m_{fc}	1kg
heat capacity of the fuel cell	C_p	750 J.kg^{-1}.K^{-1}
heat capacity of the air	$C_{p\,air}$	1000 J.kg^{-1}.K^{-1}
latent heat of vaporization	L_{H2O}	2500 kJ.kg^{-1}
natural convection coefficient	k_{nat}	0.25 W.K^{-1}
ambiant temperature	T_{amb}	25°C
high threshold temperature	T_{max}	44°C
low threshold temperature	T_{min}	41°C
oxygen stoechiometric-ratio	S_c	5

ACKNOWLEDGMENT

The research leading to these results has received funding from the European Union's Seventh Framework Programme (FP7/2007-2013) under grant agreement ETRERA 2020 num. [609543] .

REFERENCES

[1] G. Squadrito, L. Andaloro, M. Ferraro, and V. Antonucci, *Hydrogen fuel cells technology*. Woodhead Publishing Limited, 2014, ch. 16 in A. Basile and A. Iulianelli, "Advances in Hydrogen Production, Storage and Distribution".

[2] R. von Helmolt and U. Eberle, "Fuel cell vehicles: Status 2007," *Journal of Power Sources*, vol. 165, no. 2, pp. 833–843, 2007.

[3] P. Thounthong, S. Rael, and B. Davat, "Energy management of fuel cell/battery/supercapacitor hybrid power source for vehicle applications," *Journal of Power Sources*, vol. 193, no. 1, pp. 376–385, 2009.

[4] E. Uherek, T. Halenka, J. Borken-Kleefeld, Y. Balkanski, T. Berntsen, C. Borrego, M. Gauss, P. Hoor, K. Juda-Rezler, J. Lelieveld *et al.*, "Transport impacts on atmosphere and climate: Land transport," *Atmospheric Environment*, vol. 44, no. 37, pp. 4772–4816, 2010.

[5] S. Trieste, S. Hmam, J.-C. Olivier, S. Bourguet, and L. Loron, "Techno-economic optimization of a supercapacitor-based energy storage unit chain: Application on the first quick charge plug-in ferry," *Applied Energy*, vol. 153, no. 0, pp. 3 – 14, 2015, supercapacitors. [Online]. Available: http://www.sciencedirect.com/science/article/pii/S0306261915005164

[6] J.-C. Olivier, N. Bernard, S. Bourguet, and L. M. Aranguren, "Techno-economic optimization of flywheel storage system in transportation," in *Symposium de Génie Électrique 2014*, 2013.

[7] A. Veziroglu and R. Macario, "Fuel cell vehicles: state of the art with economic and environmental concerns," *International Journal of Hydrogen Energy*, vol. 36, no. 1, pp. 25–43, 2011.

[8] D. Trichet, S. Chevalier, G. Wasselynck, J. Olivier, B. Auvity, C. Josset, and M. Machmoum, "Global energy optimization of a light-duty fuel-cell vehicle," in *Vehicle Power and Propulsion Conference (VPPC), 2011 IEEE*. IEEE, 2011, pp. 1–6.

[9] G. Wasselynck, B. Auvity, J.-C. Olivier, D. Trichet, C. Josset, and P. Maindru, "Design and testing of a fuel cell powertrain with energy constraints," *Energy*, vol. 38, no. 1, pp. 414–424, 2012.

[10] J.-C. Olivier, G. Wasselynck, D. Ireena, B. Auvity, C. Josset, C. Le-Bozec, and P. Maindru, "Power source to wheel model of a high efficiency fuel cell based vehicle," in *Vehicle Power and Propulsion Conference (VPPC), 2010 IEEE*, Sept 2010, pp. 1–6.

[11] C.-J. Brodrick, T. E. Lipman, M. Farshchi, N. P. Lutsey, H. A. Dwyer, D. Sperling, S. W. Gouse Iii, D. B. Harris, and F. G. King, "Evaluation of fuel cell auxiliary power units for heavy-duty diesel trucks," *Transportation Research Part D: Transport and Environment*, vol. 7, no. 4, pp. 303–315, 2002.

[12] L. Boulon, D. Hissel, A. Bouscayrol, M.-C. Pera, and P. Delarue, "Multi physics modelling and representation of power and energy sources for hybrid electric vehicles," in *Vehicle Power and Propulsion Conference, 2008. VPPC'08. IEEE*. IEEE, 2008, pp. 1–6.

[13] G. Souffran, L. Miègeville, and P. Guérin, "Simulation of real-world vehicle missions using a stochastic markov model for optimal powertrain sizing," *Vehicular Technology, IEEE Transactions on*, vol. 61, no. 8, pp. 3454–3465, 2012.

[14] S. G. Kandlikar and Z. Lu, "Thermal management issues in a pemfc stack–a brief review of current status," *Applied Thermal Engineering*, vol. 29, no. 7, pp. 1276–1280, 2009.

[15] C. Bao, M. Ouyang, and B. Yi, "Modeling and optimization of the air system in polymer exchange membrane fuel cell systems," *Journal of Power Sources*, vol. 156, no. 2, pp. 232–243, 2006.

[16] L. Boulon, K. Agbossou, D. Hissel, P. Sicard, A. Bouscayrol, and M.-C. Péra, "A macroscopic pem fuel cell model including water phenomena for vehicle simulation," *Renewable Energy*, vol. 46, pp. 81–91, 2012.

[17] X. Li, Z.-H. Deng, D. Wei, C.-S. Xu, and G.-Y. Cao, "Parameter optimization of thermal-model-oriented control law for pem fuel cell stack via novel genetic algorithm," *Energy Conversion and Management*, vol. 52, no. 11, pp. 3290–3300, 2011.

[18] Y. Li, S. Xu, Z. Yang, and Y. Li, "Control strategy and thermal management system research of fuel cell engine in sub-freezing," in *Mechanic Automation and Control Engineering (MACE), 2011 Second International Conference on*. IEEE, 2011, pp. 4830–4833.

[19] R. F. Mann, J. C. Amphlett, M. A. Hooper, H. M. Jensen, B. A. Peppley, and P. R. Roberge, "Development and application of a generalised steady-state electrochemical model for a pem fuel cell," *Journal of Power Sources*, vol. 86, no. 1, pp. 173–180, 2000.

[20] T. V. Nguyen and R. E. White, "A water and heat management model for proton-exchange-membrane fuel cells," *Journal of the Electrochemical Society*, vol. 140, no. 8, pp. 2178–2186, 1993.

[21] Y. Lee, B. Kim, and Y. Kim, "An experimental study on water transport through the membrane of a pefc operating in the dead-end mode," *International journal of hydrogen energy*, vol. 34, no. 18, pp. 7768–7779, 2009.

[22] R. C. Eberhart and J. Kennedy, "A new optimizer using particle swarm theory," in *Proceedings of the sixth international symposium on micro machine and human science*, vol. 1. New York, NY, 1995, pp. 39–43.

[23] I. Manke, C. Hartnig, M. Grünerbel, W. Lehnert, N. Kardjilov, A. Haibel, A. Hilger, J. Banhart, and H. Riesemeier, "Investigation of water evolution and transport in fuel cells with high resolution synchrotron x-ray radiography," *Applied Physics Letters*, vol. 90, no. 17, p. 174105, 2007.

[24] C. Hartnig, I. Manke, R. Kuhn, N. Kardjilov, J. Banhart, and W. Lehnert, "Cross-sectional insight in the water evolution and transport in polymer electrolyte fuel cells," *Applied Physics Letters*, vol. 92, no. 13, p. 134106, 2008.

[25] J. Lee, J. Hinebaugh, and A. Bazylak, "Synchrotron x-ray radiographic investigations of liquid water transport behavior in a pemfc with mpl-coated gdls," *Journal of Power Sources*, vol. 227, pp. 123–130, 2013.